Over-The-Air Deramping For Multistatic Perimeter Surveillance

M. Ash, M. Ritchie, P. V. Brennan
Department of Electronic and Electrical Engineering
University College London, London, UK
Email: {m.ash, uceemri, p.brennan}@ucl.ac.uk

K. Chetty
Department of Security and Crime Science
University College London, London, UK
Email: k.chetty@ucl.ac.uk

***Abstract*—This paper explores the use of an over-the-air deramping (OTAD) system as a solution for perimeter surveillance. Over-the-air deramping is a technique for wirelessly synchronising distributed passive FMCW radar nodes to a dual-frequency master FMCW transmitter node. Such a system gives the benefits of simultaneous monostatic and multistatic measurements for improved clutter resilience, and multiple looks at a target for reduced susceptibility to signal fading due to target scintillation. To prove the latter, a simultaneous monostatic and OTAD bistatic node were set up with a 5 m baseline, and a walking person was measured. The results show that signal fading occurs in both the monostatic and the bistatic node, but rarely at the same time. Hence, combining the measurements from the two nodes gives a consistent response from the target. This demonstrates the benefit of an OTAD system for a robust perimeter surveillance system.**

***Index Terms*—FMCW radar; multistatic radar; perimeter protection.**

I. Introduction

Frequency modulated continuous wave (FMCW) radar has emerged as a widely adopted solution for low-cost systems in contemporary literature. It has many useful characteristics such as fine range resolution, good immunity to blocker/interference signals, and low peak power and sampling rate requirements [1]. Applications have included autonomous cruise control systems [2], the measurement of geophysical phenomena [3], [4] and weather radar [5]. However, these systems are all based on a familiar FMCW radar architecture, which only allows for monostatic or wired multistatic measurements [6].

The over-the-air deramping (OTAD) technique has been suggested as a low-cost method of synchronising passive FMCW nodes in [7]. OTAD has numerous benefits as a multstatic system solution. Based on FMCW radar, an OTAD system provides good range resolution, requires low peak power and it has low digital throughput requirements.

In this paper, the OTAD technique is analysed as a solution for a multistatic perimeter security radar system. The paper begins with a brief explanation of the OTAD technique and a description of how it may be used to implement a perimeter surveillance system. A field measurement, using a bistatic OTAD system, of a walking person is presented as range-versus-time and range-versus-velocity images. The results are discussed in the context of perimeter surveillance.

II. Over-The-Air Deramping

The OTAD technique was first introduced in [7] where it was described as a compelling solution for short to medium range security applications. The technique is based on the use of a super-heterodyne FMCW radar system where a linear FMCW signal is generated at an IF and converted to its operating frequency using an up-conversion process. An OTAD system taps off a portion of the IF signal in a master transmitter node and broadcasts it using some antenna with suitably wide coverage. This is known as the reference chirp signal. The signal is simultaneously directed towards a target scene at the radar operating frequency.

The OTAD receivers can be purely passive, with a reference chirp receiver channel and a target echo channel. The reference chirp is collected with a directive antenna that is pointed towards the master node. This signal is filtered and amplified to a level that can drive a deramp mixer. The target echo is simultaneously collected and down-converted, before deramping with the amplified reference chirp signal. A multistatic OTAD system can easily be arranged to surveil a perimeter, as shown in Fig. 1, at low-cost. As a multistatic system, it also has increased resilience to clutter, and multiple looks at a target for an improved chance of correct classification [8]. Furthermore, using a dual-frequency design, OTAD avoids the problem of direct signal interference usually associated with passive bistatic nodes [9].

Using a similar analysis as Stove [1], over-the-air deramping involves mixing the target signal (assumed to be ideally converted from operating frequency to IF) and the over-the-air deramp signal y_d as follows:

$$\begin{aligned} y_d(t) &= x_s(t) \cdot x_t(t) \\ y_d(t) &= g_o \cos 2\pi [f_o (\tau_t - \tau_s) + \alpha t (\tau_t - \tau_s) \\ &\qquad - (1/2)\alpha (\tau_t^2 - \tau_s^2)] \end{aligned} \quad (1)$$

where f_o is the operating frequency, α is the linear chirp rate, and τ_t and τ_s are the propagation delays of the target echo signal and the reference chirp signal respectively.

Hence the deramp frequency becomes a function of the propagation delay between the master and slave nodes, or baseline distance, and the bistatic path. Furthermore, the range

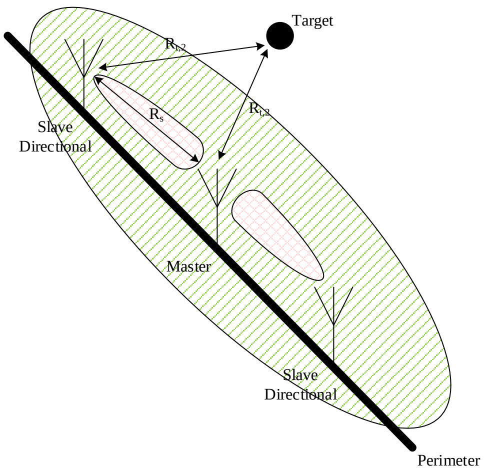

Fig. 1. Diagram of a OTAD system for perimeter surveillance.

measurement to the target is the bistatic range, that is the combination of the path from the transmitter to the target and the path from the target to the receiver as shown in Fig. 1. Hence, R_t is a simplification of bistatic range $R_{t,1} + R_{t,2}$ whose inclusion modifies the deramp frequency to

$$\begin{aligned} f_d &= \alpha(\tau_t - \tau_s) \\ f_d &= \frac{B(R_{t,1} + R_{t,2})}{cT} - \frac{BR_s}{cT} \end{aligned} \tag{2}$$

The expression of the OTAD deramp signal in Equation (1) can be expanded to include relative motion, v, of a target in the field of view, i.e. $\tau_t = 2r_t/c + 2vt/c$, thus

$$\begin{aligned} y_d(t) = g_o \cos 2\pi \Bigg[&\frac{2f_o}{c}(r_t - r_s) + \frac{2\alpha}{c}(r_t - r_s)\,t \\ &+ \frac{2f_o vt}{c} + \frac{2\alpha vt^2}{c} \Bigg] \end{aligned} \tag{3}$$

where it has been assumed that the two radar nodes have zero relative motion, and the third term of Equation (1) can be ignored assuming that the propagation time delay is much less than the chirp period, i.e. $\tau_t \ll T; \tau_s \ll T$. The third term of Equation (3) can be estimated from measurements using triangular modulation of the chirp waveform or two-dimensional Fourier analysis [10]. The fourth term expresses delay-Doppler cross-coupling [1]. Once again, expanding R_t, the moving target deramp frequency is

$$f_d = \frac{B(R_{t,1} + R_{t,2})}{cT} - \frac{BR_s}{cT} + \frac{2f_o v}{c} \tag{4}$$

With the locations of the nodes known, curves of constant range can be plotted for each master-slave node pair giving an precise measurement of target location and velocity vector. The final aper will include an example of this localisation from the measurements described in Section IV. This makes the OTAD technique well-suited to perimeter surveillance.

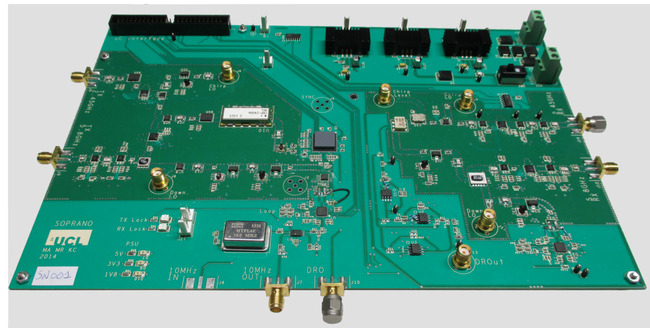

Fig. 3. Soprano FMCW OTAD radar PCB.

III. Soprano System

Soprano is a unique, PCB-based FMCW system developed at UCL for testing the OTAD technique. A high-level block diagram of its design is shown in Fig. 2. The system operates in the 2.4GHz and 5.8GHz ISM bands for broadcasting the reference chirp signal and the radar signal respectively. The waveform bandwidth is limited to $83.5\,\text{MHz}$ to adhere to UK Ofcom regulations, however wider bandwidths are possible with the design. The transmit power is $+13\,\text{dBm}$ and the receiver nominal noise figure is $2.5\,\text{dB}$, not accounting for losses in antenna and PCB interconnecting cables.

The system can be programmed to operate as a conventional monostatic FMCW tranceiver, known as a master node, or as a passive bistatic FMCW receiver, known as a slave node. To date, two Soprano PCB's have been constructed, hence simultaneous monostatic and bistatic measurements are possible and have been reported in [7].

It can be seen that the downconversion process in the transmitter and the receiver nodes operates on separate reference clocks. This causes a time-varying mismatch in frequency that is captured by the deramp signal as follows:

$$\begin{aligned} y_d(t) = d_o \cos 2\pi \big[&f_o\tau_t + \alpha\tau_t t - (1/2)\alpha\tau_t^2 \\ &+ \Delta f_{LO}(t) t \big] \end{aligned} \tag{5}$$

where $\Delta f_{LO}(t)$ is the time-varying frequency error. This can be corrected for by estimating the frequency error using the reflection from a bright, stationary target as suggested in [7] (direct signal from the transmitted could also be used, however this is filtered in the baseband frequency-gain control filter prior to digitisation in the Soprano system). Following correction, the system is capable of recording multistatic range, velocity and micro-Doppler measurements.

IV. Field Measurements

The OTAD technique has the advantage of providing simultaneous monostatic and multistatic measurements of targets.

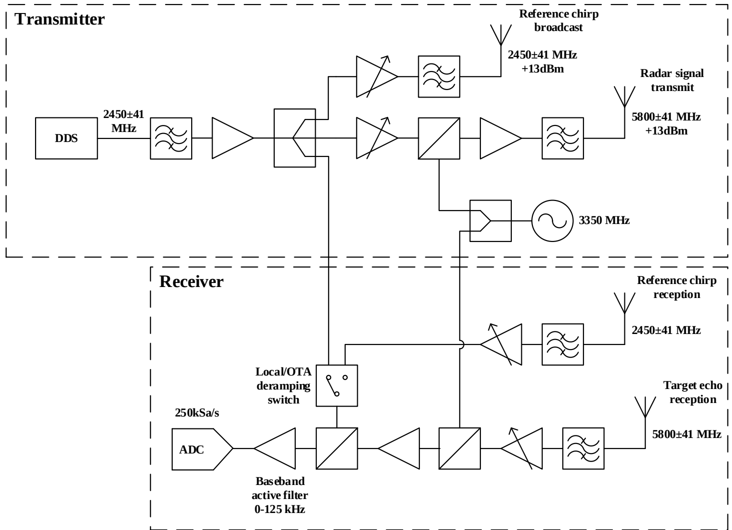

Fig. 2. Simplified system block diagram of Soprano FMCW OTAD radar.

TABLE I
SOPRANO FMCW OTAD RADAR SPECIFICATION.

Centre Frequency	5.8 GHz
Transmit Power	13 dBm
Waveform Bandwidth	83.5 MHz
Base-bandwidth	125 kHz
Noise Fig.	2.5 dB
Phase Noise	
@ 1 kHz	−83 dBm/Hz
@ 100 kHz	−85 dBm/Hz
@ 1 MHz	−125 dBm/Hz

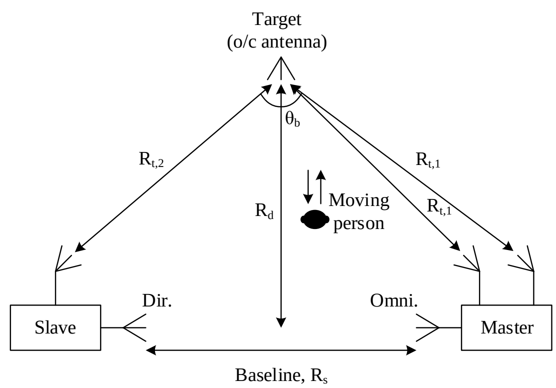

Fig. 4. Diagram of experiment setup.

With the available Soprano hardware, monostatic and bistatic measurements are possible. To demonstrate the gain provided by an OTAD system in terms of target localisation and resilience to target scintillation, some field measurements with Soprano was taken. The measurement presented in this paper is of a person walking from the centre of the master-slave baseline ($R_d = 0$ m), towards a stationary target (an open-circuited, 30° antenna) at $R_d = 50$ m, and back again.

Two Soprano radar nodes were used in the experiments; one was configured as a master node and the other as a slave node. The two nodes were separated to give a baseline, R_s, of 5 m forming a bistatic angle range of 90° and 5.7° between 2.5 and 50 m. Fig. 4 shows a diagram of the experiment setup.

The transmit power was kept at its maximum level (+13 dBm). The chirp period was set to 1 ms and bandwidth to 83.5 MHz, and a sawtooth modulation scheme was used (i.e. up-chirps only). Such waveforms give a nominal range resolution of 1.8 m. The over-the-air deramp signal was broadcast using a c. 2 dBi horizontally omnidirectional antenna and the chirp-facing antenna on the slave node had a gain of c. 12 dBi. Each of the 5.8 GHz radar channel antennas were 30° yagi antennas with a gain of 12 dBi. The antennas were mounted 1.5 m above the ground.

Fig. 5 shows a range-versus-time image of the walking person. These images are produced following moving-target-indication filtering. Additionally, the frequency mismatch in the bistatic OTAD data described by Eq. (5) has been corrected using a stationary target within the field-of-view, as described in [7].

Fig. 6 shows an image of a sample of the spectrogram, that is velocity-versus-time, of the walking person data. It can be seen in Fig. 6a that there is a fade in the signal seen by the master monostatic node. This is due to target scintillation as the radar-to-target geometry, and therefore look angle, varies with time. By employing the OTAD technique in the form of a bistatic pair, the system would be able to overcome this particular issue. Fig. 6b shows that the fade in signal is not present in the view of the bistatic OTAD node.

In this case, the signal fade lasts just over 1 s, which is not a terminal period of time for an target moving at these

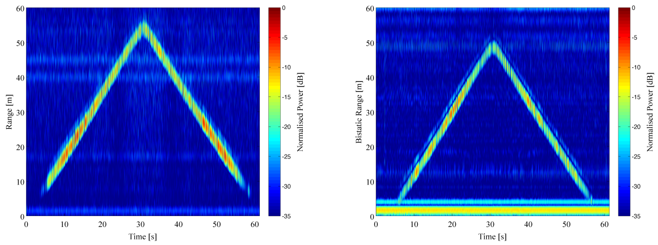

(a) (b)

Fig. 5. Range-versus-time image of person walking away from and towards the radar baseline from the perspective of (a) the master monostatic node, and (b) the slave bistatic OTAD node.

speeds. However, for a target approaching at faster speeds, signal fades of this duration become more of an issue. This shows the benefit of using a spatially-diverse bistatic OTAD system.

In this dataset, there are also instances when fading affects the bistatic OTAD node and not the monostatic node. There is also a case where both nodes experience fading for some 1 s. It has been shown that with system comprised of multiple distributed radar nodes, the susceptibility of the system to fading can be reduced [11]. Hence, the appearance of signal fades with the bistatic OTAD system currently used in this measurements can be improved with the addition of more bistatic OTAD nodes. The approach of increasing the number of passive OTAD nodes is visualised in Fig. 1 for a multistatic perimeter surveillance system.

V. Conclusions and Future Work

In this paper, we have discussed the use of the over-the-air deramping technique for perimeter surveillance. The technique allows for the synchronisation of distributed passive FMCW nodes which allows for spatially diverse surveillance of a perimeter. A simultaneous monostatic and OTAD bistatic measurement of a walking person has been shown. The angular diversity that the OTAD technique provides has been shown to reduce the susceptibility of the system to signal fading from target scintillation. This makes the OTAD technique a good solution for a perimeter surveillance system.

Acknowledgment

The authors would like to thank the UCL Institute of Making for funding the hardware component of this project through the EPSRC Bridging the Gaps grant. Matthew Ash would like to further thank the EPSRC for their support of his research through grant ref. EP/K00767X/1.

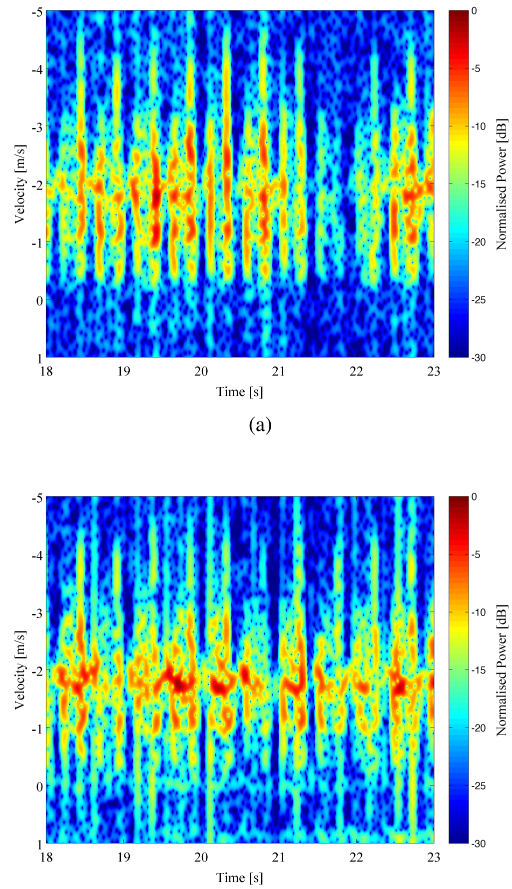

(b)

Fig. 6. Sample of the spectrogram, that is velocity-versus-time, of the of the human walking person data plotted in Fig. 5 from the perspective of (a) the master monostatic node, and (b) the slave bistatic OTAD node.

References

[1] A. Stove, "Linear FMCW radar techniques," *IEE Proceedings For Radar and Signal Processing*, vol. 139, no. 5, pp. 343–350, 1992.

[2] C. Hu, Y. Liu, H. Meng, and X. Wang, "Randomized switched antenna array fmcw radar for automotive applications," *IEEE Transactions on Vehicular Technology*, vol. 63, no. 8, pp. 3624–3641, Oct 2014.

[3] M. Ash, P. V. Brennan, C. J. Keylock, N. M. Vriend, J. N. McElwaine, and B. Sovilla, "Two-dimensional radar imaging of flowing avalanches," *Cold Regions Science and Technology*, vol. 102, pp. 41 – 51, 2014.

[4] P. Brennan, L. Lok, K. Nicholls, and H. Corr, "Phase-sensitive fmcw radar system for high-precision antarctic ice shelf profile monitoring," *IET Radar, Sonar & Navigation*, vol. 8, no. 7, pp. 776–786, Aug 2014.

[5] D. Gray, M. Viola, W. Moran, S. Samarasekera, P. May, B. Bates, K. Venkataraman, C. McCarroll, B. Ferguson, and D. McLaughlin, "WREN: A weather radar experimental network," in *International Conference on Electromagnetics in Advanced Applications (ICEAA), 2010*, Sept 2010, pp. 505–508.

[6] P. Sammartino and J. Fortuny-Guasch, "Space and frequency diversity for moving personnel spectrogram estimation," in *IEEE Radar Conference, 2010*, May 2010, pp. 374–379.

[7] M. Ash, M. Ritchie, K. Chetty, and P. V. Brennan, "A new multistatic fmcw radar architecture by over-the-air deramping," *IEEE Sensors Journal*, vol. (submitted), 2015.

[8] P. Stinco, M. Greco, F. Gini, and M. Manna, "Non-cooperative target recognition in multistatic radar systems," *IET Radar, Sonar & Navigation*, vol. 8, no. 4, pp. 396–405, April 2014.

[9] J. Brown, K. Woodbridge, H. Griffiths, A. Stove, and S. Watts, "Passive bistatic radar experiments from an airborne platform," *IEEE Aerospace and Electronic Systems Magazine*, vol. 27, no. 11, pp. 50–55, November 2012.

[10] A. Hymans and J. Lait, "Analysis of a frequency-modulated continuous-wave ranging system," *Proceedings of the IEE - Part B: Electronic and Communication Engineering*, vol. 107, no. 34, pp. 365 –372, July 1960.

[11] A. Haimovich, R. Blum, and L. Cimini, "Mimo radar with widely separated antennas," *Signal Processing Magazine, IEEE*, vol. 25, no. 1, pp. 116–129, 2008.